Journal of Physiology (2002), **542.3**, *pp.* 685–697
DOI: 10.1113/jphysiol.2002.018978

www.jphysiol.org

Functional glycine receptor maturation in the absence of glycinergic input in dopaminergic neurones of the rat substantia nigra

J. M. Mangin, A. Guyon, D. Eugène, D. Paupardin-Tritsch and P. Legendre

UMR CNRS 7102 Neurobiologie des Processus Adaptatifs, Université Pierre et Marie Curie, 9 Quai St Bernard, 75252 Paris cedex 05, France

The postnatal maturation pattern of glycine receptor channels (GlyRs) expressed by dopaminergic (DA) neurones of the rat substantia nigra pars compacta (SNc) was investigated using single-channel and whole-cell patch-clamp recordings in brain slices from rats aged 7–21 postnatal days (P). In neonatal rats (P7–P10), GlyRs exhibited a main conductance state of 100–110 pS with a mean open time of 16 ms. In juvenile rats (P19–P22), both the GlyR main conductance state (46–55 pS) and the mean open time (6.8 ms) were decreased. In neonatal rats, application of 30 μM picrotoxin, which is known to block homomeric GlyRs, strongly reduced glycine-evoked responses, while it was much less effective in juvenile rats. These results suggest that these GlyRs correspond functionally to α_2 homomeric GlyRs in neonatal rats and α_1/β heteromeric GlyRs in juvenile rats. A drastic but transient decrease in the glycine responsiveness of DA neurones occurred around P17 concomitant to the functional switch from the homomeric state to the heteromeric state. This age corresponds to a maturation phase for DA neurones. The application of 1 μM gabazine blocked spontaneous or evoked inhibitory synaptic current, while the addition of 1 μM strychnine had no effect, suggesting a lack of functional glycinergic synapses on DA neurones. Although it has been proposed that taurine is co-released with GABA at GABAergic synapses on DA neurones, in the present study the stimulation of GABAergic fibres failed to activate GlyRs. Blockade of taurine transporters and applications of high K^+ and hyposmotic solutions were also unable to induce any strychnine-sensitive current. We conclude that functional maturation of GlyRs can occur in the absence of any detectable GlyR activation in DA neurones of the SNc.

(Received 18 February 2002; accepted after revision 9 May 2002)
Corresponding author J. M. Mangin: UMR CNRS 7102 Neurobiologie des Processus Adaptatifs, Université Pierre et Marie Curie, Batiment B, 3 étage, 9 quai St Bernard, 75252 Paris cedex 05, France. Email: jmmangin@snv.jussieu.fr

The glycine receptor (GlyR) is a ligand-gated anionic channel that is primarily involved in fast inhibitory synaptic transmission (for review see Legendre, 2001). GlyRs are pentameric transmembrane proteins for which two different subunits have been characterized so far, an α subunit (48 kDa) and a β subunit (58 kDa). Molecular studies of GlyR subunits in the rat have revealed the existence of four different isoforms for the α subunit (α_1–α_4) and only one β isoform. GlyRs can assemble functionally either into a homomeric form composed of five α subunits, or into a heteromeric form composed of three α and two β subunits (Langosch *et al.* 1988). GlyR expression is regulated during development: the α_2 subunit is expressed predominantly in fetuses and neonatal rats and is progressively replaced by the α_1 subunit during the second postnatal week in most structures (Akagi & Miledi, 1988; Malosio *et al.* 1991). In addition, α homomeric GlyRs are predominant during fetal and early postnatal development, whereas adult GlyRs are essentially α/β heteromeric GlyRs (Becker *et al.* 1988; Takahashi *et al.* 1992; Kaneda *et al.* 1995; Kungel & Friauf, 1997; Flint *et al.* 1998; Ye, 2000). These observations have lead to the maturation model of the glycinergic synapse consisting of the progressive replacement of α_2 homomeric GlyRs by α_1/β heteromeric GlyRs during brain development (Vannier & Triller, 1997; Kneussel & Betz, 2000; Legendre, 2001).

The crucial role of glycinergic afferents in the recruitment of gephyrin and α/β heteromeric GlyRs at postsynaptic densities has been documented extensively (Kneussel & Betz, 2000). However, the role of the glycinergic inputs and/or GlyR activation in the maturation from α homomeric to α/β heteromeric GlyR remains controversial. To address this issue, GlyR maturation events must be analysed on neurones lacking any specific glycinergic synapses.

Dopaminergic (DA) neurones of the substantia nigra pars compacta (SNc) are known to express functional GlyRs that can be activated by either exogenous application of glycine or of taurine, a GlyR agonist (Mercuri *et al.* 1988; Hausser *et al.* 1992). The presence of glycinergic afferents in the substantia nigra is unlikely considering the very

small number of glycine-immunoreactive fibres (Rampon *et al.* 1996) as well as the absence of both the synaptic glycine transporter GLYT2 protein and its mRNA (Zafra *et al.* 1995). However, high levels of taurine and a high-affinity uptake system for taurine have been observed in the substantia nigra (Clarke *et al.* 1983; Allen *et al.* 1986), and taurine could be physiologically co-released with GABA from striatonigral afferents (Bianchi *et al.* 1998). Accordingly, taurine release could activate the GlyRs expressed by DA neurones if GlyRs were co-localized with $GABA_A$ receptors at the same synapse, as is observed in the brainstem and spinal cord (Todd *et al.* 1996; O'Brien & Berger, 1999).

Here, we have examined the functional and pharmacological properties of GlyRs during the postnatal development of DA neurones of the SNc from rats aged from 7–22 days, by means of whole-cell and outside-out patch-clamp techniques. Our results demonstrate a switch from the α homomeric state to the α/β heteromeric state in DA neurones, correlated with a transient gap in GlyR expression at postnatal day (P) 17. However, we have observed that the DA neurone GlyRs could not be activated at any of these developmental stages by either spontaneous or evoked synaptic activity.

METHODS

The experiments conform with the European Community guiding principles in the care and use of animals (86/609/CEE, CE official journal no. L358, 18 December 1986), French decree no. 97/748 of 19 October 1987 (J Off République Française, 20 October 1987, pp. 12245–12248) and the recommendation of CNRS and University Paris VI.

Slice preparation

Male Wistar rat pups (P7–P22) were anaesthetized with halothane prior to decapitation. The brains were then quickly removed and placed in ice-cold phosphate–bicarbonate-buffered solution (PBBS) composed of (mM): 125 NaCl, 2.5 KCl, 0.4 $CaCl_2$, 1 $MgCl_2$, 25 glucose, 1.25 NaH_2PO_4, 26 $NaHCO_3$, and bubbled with 95 % O_2–5 % CO_2 (pH 7.4). Three or four coronal or horizontal slices (200–350 μm thick) containing the SNc were cut from the midbrain with a microslicer VT1000S (Leica, Germany), transferred to an incubating chamber maintained at 32–35 °C and continuously superfused with oxygenated PBBS for 1 h. These slices were then used for patch-clamp recording of DA neurones for 5–6 h.

Patch-clamp recording

Slices were placed under a Nomarski optic microscope (Nikon, France) in a recording chamber superfused at a flow rate of 1 or 2 ml min^{-1} with oxygenated PBBS containing additional $CaCl_2$ (final concentration: 2 mM). All whole-cell and single-channel patch-clamp recordings were made at room temperature using an Axopatch 200B amplifier (Axons Instruments, USA). Currents were filtered at 10 kHz (four-pole low-pass Bessel filter) and recorded on digital audiotape (DTR-1204; Biologic, France). Patch pipettes were made from borosilicate capillary glass (Hilgenberg, Germany), coated with dental wax or Sylgard resin (Rhône-Poulenc, France) and fire-polished to obtain a resistance of 3–5 MΩ for whole-cell recordings and 5–10 MΩ for single-channel recordings. The pipettes were filled with a solution containing (mM): 137 CsCl, 5 $MgCl_2$, 1 $CaCl_2$, 10 EGTA, 4 Na-ATP, 0.4 Na-GTP, 10 Hepes (pH adjusted to 7.3 with CsOH, osmolarity 290 mosmol l^{-1}).

During whole-cell recordings, values of access resistance ranged from 3 to 15 MΩ and were compensated at 75–80 %. The value of the access resistance was checked repeatedly during each experiment. Measurements were performed 2–3 min after obtaining the whole-cell configuration to ensure cell dialysis. During outside-out recordings, values of seal resistance ranged from 2 to 20 GΩ and patches were recorded during 15–20 min after excision.

Chemicals and drug solutions

Picrotoxin, strychnine, SR-95531 (gabazine), 6-cyano-7-nitro-quinoxaline-2,3-dione (CNQX) and DL-2-amino-5-phosphono-valeric acid (DL-APV) were obtained from Sigma-RBI (USA). Glycine and taurine were obtained from Tocris (USA). Guanidino-ethyl sulfonate (GES) was obtained from Toronto Research Chemicals (Canada). Concentrated stock solutions of 1 mM gabazine and 10 mM DL-APV were prepared in distilled water and stored at −20 °C. A stock solution of 1 mM CNQX in distilled water was prepared in the presence of 15 mM cyclodextrin (RBI, USA) in order to dissolve CNQX (Pitha, 1985). All stock solutions were diluted to the appropriate concentration just before the experiment. All other drug solutions were made freshly on the day of the experiment. Drugs were diluted in PBBS, except for single-channel recordings for which drugs were diluted in Hepes-buffered solution composed of (mM): 150 NaCl, 2.5 KCl, 2 $CaCl_2$, 1 $MgCl_2$, 20 glucose, 10 Hepes (pH adjusted to 7.2 with NaOH, osmolarity 290 mosmol l^{-1}).

Drug delivery

Drug solutions were applied via a multi-barrelled application system composed of six horizontally aligned quartz tubes (inside diameter 250 μm; outside diameter 350 μm; Polymicro Technologies). Solution exchange was achieved by lateral movements performed by a mechanical translator (Melles Griot, France) that allowed a complete solution exchange in 500–1000 ms. Drugs were delivered by bath application in experiments in which a stimulation electrode was used.

Electrical stimulation

Synaptic activity was evoked with single electrical stimuli applied through a glass pipette (tip diameter between 20 and 40 μm) filled with external PBBS solution. The current intensity of the stimulation was controlled using an isolation unit (Weco). In some experiments, stimulation trains of five stimuli spaced by 3 ms intervals were applied. The stimulation pipette was placed into the substantia nigra pars reticularis and the optimal stimulation was obtained by scanning an area 400–600 μm from the recorded cell. The stimulation frequency (0.05 Hz) and the pulse duration (100 μs) were monitored using a PC computer running pCLAMP 5.5 software (Axon Instruments).

Electrophysiological data analysis

Stimulation experiments were acquired online using a Labmaster interface coupled to a PC computer running pCLAMP version 5.5 software. Other experiments were acquired offline by replaying recordings from a digital audiotape. Data were then transferred to a G4 Macintosh computer to be visualized and analysed using Axograph 4.6 (Axon Instruments). Whole-cell recordings were digitized at 10 kHz and digitally filtered at 1 kHz, whereas single-channel currents were digitized at 25 kHz and digitally filtered at 2–3 kHz.

Table 1. Occurrence of the different conductance levels of glycine receptors during postnatal development

Postnatal age (days)	Level I 100–110 pS	Level II 82–90 pS	Level III 65–70 pS	Level IV 46–55 pS	Level V 28–32 pS
7–10	20/33 (60 %)	15/33 (45 %)	8/33 (24 %)	32/33 (97 %)	13/33 (39 %)
13–16	1/15 (7 %)	7/15 (46 %)	3/15 (20 %)	15/15 (100 %)	6/15 (40 %)
19–22	0/15 (0 %)	1/15 (7 %)	0/15 (0 %)	14/15 (93 %)	10/15 (66 %)

Values indicated for each level correspond to the number of patches where this level was observed *versus* the total number of patches recorded at the three different stages (postnatal days (P)7–P10, P13–P16 and P19–P22). Corresponding percentages are indicated below each value.

Time courses of inhibitory postsynaptic currents (IPSCs) evoked by electrical stimulation were analysed by averaging 10 responses in each condition. The first 100 ms of the decay phase was fitted with a sum of exponential curves using Axograph 4.6. The presence of one or two exponential components was tested by comparing the sum of squared errors (SSEs) of the fits.

The analysis of the evoked single-channel openings was performed by selecting patches with a low frequency of openings to avoid overlapping events. Single-channel current levels were determined using point-per-point amplitude histograms obtained from recording epochs of 25–50 s. Amplitude histograms were fitted with a sum of Gaussian functions, using the least square method (Simplex algorithm). The optimal number of Gaussian functions was determined by comparing the SSEs of the different multi-Gaussian fits. The different conductance levels were defined from the mean current amplitude of each Gaussian function and the theoretical E_{Cl} (−2 mV). The relative proportion of time spent in each level was given by the relative area of each Gaussian function. The charge transferred was calculated by weighting the Gaussian function area by the mean amplitude given by the Gaussian fit. Dwell times were analysed using the semi-automatic 'event-list' algorithm of Fetchan software (Axon Instruments), which uses a threshold-crossing procedure. Care was taken to systematically exclude opening summation by manually processing each trace analysed. Dwell-time distribution histograms were then constructed using pStat (pCLAMP 6.0, Axon Instruments). Dwell-time histograms showing the distributions in log intervals with the ordinate on a square root scale (Sigworth & Sine, 1987) were fitted to the sum of several exponential curves using the least square method. The mean open time (τ_m) was calculated from the time constant of each exponential component (τ_1, τ_2 and τ_3) and their relative amplitude (a_1, a_2 and a_3) as follows: $\tau_m = \tau_1 a_1 + \tau_2 a_2 + \tau_3 a_3$.

Averaged data are expressed as mean ± S.D., except when stated otherwise. The number of neurones or patches pooled is given by *n*. Statistical significance of the data was assessed from a Student's *t* test or analysis of variance (ANOVA) followed by Dunnet's multiple-comparison post tests (DMCT) when significance was reached.

RESULTS

Changes in single-channel properties of GlyRs during postnatal development

To determine possible changes in native GlyR subtypes during postnatal development, we studied GlyR single-channel conductances and kinetics in outside-out patches excised from DA neurones taken from animals aged between P7 and P22. It has been shown that all GlyRs exhibit multiple-conductance chloride channels during single-channel recordings (Hamill *et al.* 1983; Bormann *et al.* 1993), the conductance state most frequently observed depending on the GlyR subunit combination. These main conductance states are respectively 110 pS, 90 pS and 50 pS for α_2 homomeric, α_1 homomeric and α/β heteromeric GlyRs (Bormann *et al.* 1993). In addition, the GlyR subunit composition has a clear influence on channel kinetics: GlyRs containing α_2 have a longer mean open time than GlyRs containing α_1, and thus the switch from the α_2 to the α_1 subunit during postnatal development is accompanied by a shortening of the mean open time (Takahashi *et al.* 1992; Singer *et al.* 1998).

Unitary currents evoked by glycine in DA neurones exhibited at least five distinct conductance levels during postnatal development (see Fig. 1 and Table 1). Level I (100–110 pS), level II (82–90 pS) and level IV (46–55 pS) were observed in 21, 23 and 61 patches, respectively ($n = 63$, see Table 1), and represented 12 %, 25 % and 60 %, respectively, of the total open time recorded. Levels III (65–70 pS) and V (30–36 pS) were observed in 11 and 29 patches, respectively ($n = 63$, see Table 1), but represented a very small proportion of the total open time (less than 5 %). Levels III and V also occurred as a direct transition from higher conductance levels (see Fig. 1, 1st and 4th traces), suggesting that they were essentially subconductance states, as shown in others studies (Takahashi *et al.* 1992; Bormann *et al.* 1993). In contrast, levels I, II and IV were similar to the main conductance states of respectively α_2 homomeric, α_1 homomeric and α/β heteromeric GlyRs expressed in human embryonic kidney (HEK)-393 cells (Bormann *et al.* 1993). As shown in Fig. 2, the relative proportion of these three main conductance levels changed during postnatal development. In neonatal rats aged between P7 and P10 (Fig. 2*A*, 13 patches pooled), level I and level IV were most frequently observed and represented 38 % and 34 % of the total open time, respectively. Level II

was also clearly present in recordings and represented 28 % of the total open time. In rats aged between P13 and P16 (Fig. 2*B*, 11 patches pooled), level II (46 % of the total open time) became predominant relative to level I (3 %), whereas the relative occurrence of level IV increased (51 %). In juvenile rats, between P19 and P22 (Fig. 2*C*, 5 patches pooled), the relative repartition of GlyR conductance levels was markedly modified with respect to the earlier stages: level IV became predominant and represented 96 % of the total open time, and only a small proportion of level II remained (4 %). This shift from highest conductance levels (levels I and II) to a lower one (level IV) suggests the existence of a developmental regulation of the GlyR functional phenotype in DA neurones.

The kinetic properties of the highest conductance level (level I) predominantly observed in neonatal rats differed greatly from those of the lower conductance level (level IV) predominantly observed in juvenile rats, as illustrated for two individual patches in Fig. 3. Similarly to what was observed in individual patches, mean time constants of the openings (τo) differed in neonatal and in juvenile rats: $\tau o_1 = 0.17 \pm 0.16$ ms and $\tau o_2 = 18.9 \pm 2.7$ ms for level I in neonates (6 patches), and $\tau o_1 = 0.5 \pm 0.3$ ms and $\tau o_2 = 9.6 \pm 4$ ms for level IV observed in juveniles (7 patches). Relative amplitudes of τo_1 and τo_2 were 15 ± 4 % and 85 ± 4 %, respectively, in neonates (level I), and 31 ± 9 % and 69 ± 9 %, respectively, in juveniles (level IV). This corresponds to a decrease in the mean open time (τ_m) from 16 ± 2.3 ms in neonates to 6.8 ± 3.3 ms in juveniles. These τ_m values, together with their decrease with age, are similar to what is observed for GlyRs in spinal cord and brainstem neurones, and probably reflect the switch from the α_2 to the α_1 GlyR subunit (Takahashi *et al.* 1992; Singer *et al.* 1998; Ali *et al.* 2000).

The observation of a large main conductance level in neonates suggests strongly the presence of α homomeric GlyRs. To confirm this hypothesis, we have measured the effect of picrotoxin on GlyR-channel activity. Picrotoxin is known to preferentially block homomeric GlyRs at concentrations below 100 μM (Legendre & Korn, 1994; Pribilla *et al.* 1994; Legendre, 1997; Tapia & Aguayo, 1998; Yoon *et al.* 1998). The effect of 30 μM picrotoxin was tested on the unitary currents evoked by 30 μM glycine applied to outside-out patches from DA neurones. At this picrotoxin

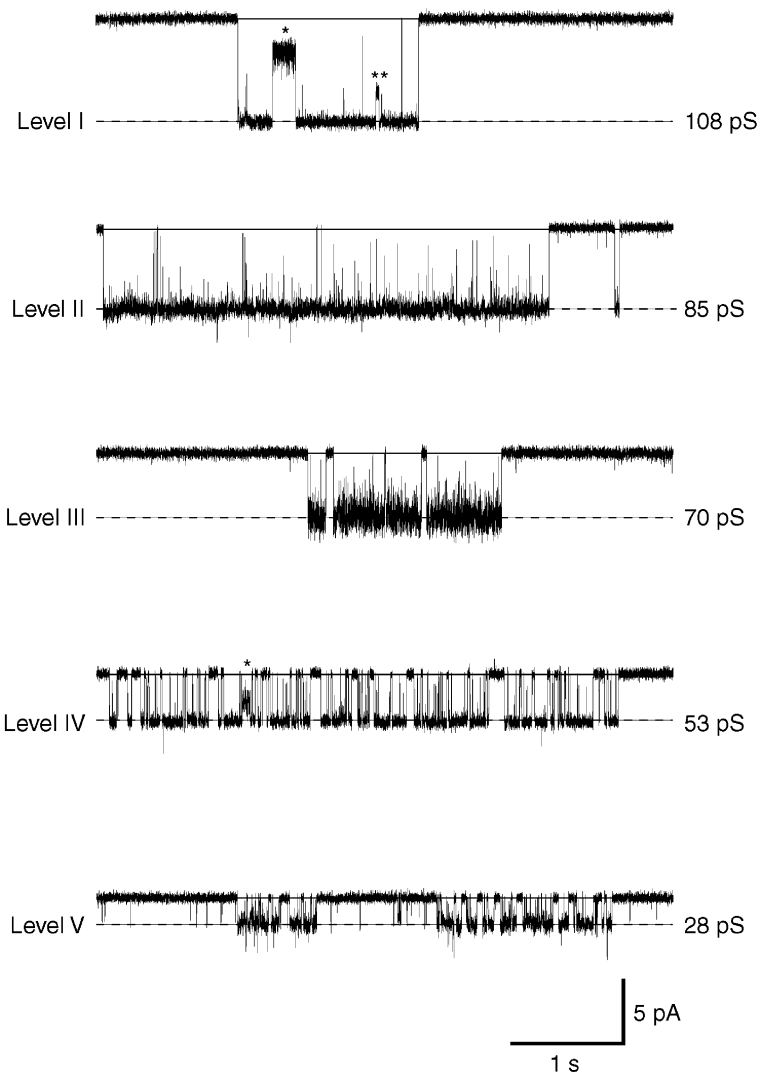

Figure 1. Conductance states of glycine receptors (GlyRs) expressed by dopamine (DA) neurones of the substantia nigra pars compacta (SNc)

Application of glycine on outside-out patches excised from DA neurones of the SNc evoked unitary currents with multiple-conductance states (holding potential, $V_H = -70$ mV). The conductance levels are marked by dotted lines and labelled from the highest level (I) to the lowest one (V). Chord conductance values indicated for each level were estimated by Gaussian fit of the point-per-point amplitude histograms obtained from the traces displayed. From all recordings, five distinct levels were distinguished, which are classified into five range levels: 100–110 pS (level I), 82–90 pS (level II), 65–70 (level III), 46–55 pS (level IV) and 28–32 pS (level V) according to the classification of Bormann *et al.* (1993). Traces were sampled at 25 kHz and filtered at 2 kHz, and correspond to epochs from longer recordings obtained from different patches. Note the direct transitions from level I to levels III and V (* and ** on the first trace) and from level IV to level V (* on the fourth trace).

concentration, the discrimination between homomeric and heteromeric states is thought to be optimal, considering the near-complete block reported for homomeric GlyRs compared to the small flickering observed for heteromeric GlyRs (Legendre & Korn, 1994; Lynch *et al.* 1995; Yoon *et al.* 1998). In neonatal rats, high-conductance levels I and II were indeed blocked by 30 μM picrotoxin (Fig. 4), the total charge transferred being decreased by 66 ± 15 % (n = 6). In contrast, in juvenile rats, picrotoxin induced a flickering of the main conductance level (level IV) corresponding to a 24 ± 8 % decrease of the total charge transferred, significantly different from the decrease observed in neonates (n = 4, unpaired t test, $P < 0.01$). Picrotoxin also significantly decreased conductance level IV by 15 ± 7 % from 52 ± 4 pS to 43 ± 3 pS (n = 4, paired t test, $P < 0.01$). The picrotoxin sensitivity of high-conductance levels confirms that they represent homomeric GlyR activation, whereas the relative insensitivity of the low-conductance levels suggests that they probably correspond to heteromeric GlyRs.

Postnatal changes in the whole-cell currents evoked by glycine

In order to determine whether this switch concerns all GlyRs in DA neurones, whole-cell currents evoked by 100 μM glycine as well as their inhibition by 30 μM picrotoxin were compared between DA neurones obtained from animals aged P7–P20 (Fig. 5*A*). The membrane capacitance of DA neurones slightly increased in this period from 26 ± 7 pF (n = 16) at P7 to 34 ± 6 pF (n = 19) at P15–P17 and further to 37 ± 9 pF (n = 7) at P20. To determine whether any change in GlyR density occurred at the cell membrane during development, we analysed changes in the current density (pA pF^{-1}). The mean current density was 19 ± 8.7 pA pF^{-1} (n = 16) at P7; this decreased significantly to 7.4 ± 7.3 pA pF^{-1} (n = 13, ANOVA-DMCT, $P < 0.001$) at P15 and further to 2.6 ± 1.6 pA pF^{-1} (n = 6, ANOVA-DMCT, $P < 0.001$) at P17, but then increased again to 19.6 ± 5 pA pF^{-1} (n = 7) at P20 (Fig. 5*B*). This result suggests that a transient decrease in GlyR density occurs around P17.

As illustrated in Fig. 5*C*, the mean percentage inhibition evoked by 30 μM picrotoxin remains stable up to P17, with values of 48 ± 15 % at P7 (n = 16), 54 ± 7 % at P15 (n = 13) and 49 ± 20 % at P17 (n = 6). By contrast, at P20, the picrotoxin sensitivity of the glycine current was significantly reduced to only 14 ± 7 % inhibition (n = 7, ANOVA-DMCT, $P < 0.001$) compared to the three other ages. These data confirm a developmental regulation of GlyR functional characteristics in DA neurones. Such changes in GlyR functional properties have already been described in other preparations where synaptic contacts are present (Takahashi *et al.* 1992; Kungel & Friauf, 1997; Tapia & Aguayo, 1998; Ali *et al.* 2000).

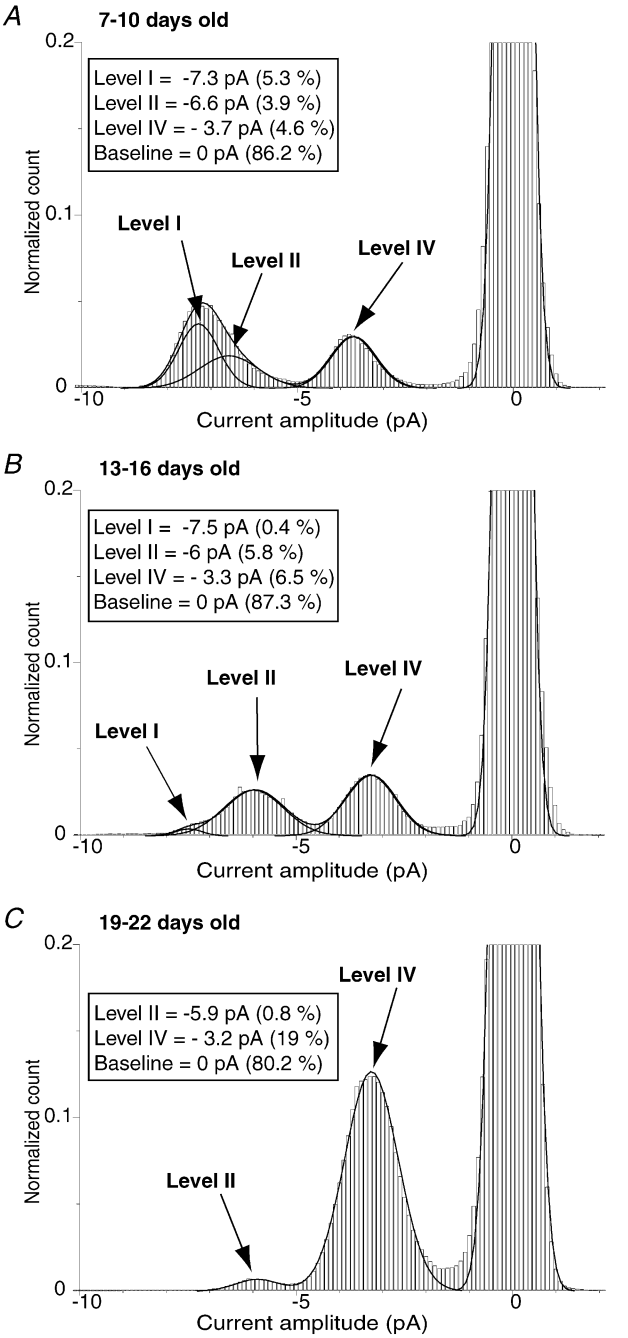

Figure 2. Developmental changes in the repartition of GlyR conductance levels

Point-per-point amplitude histograms of unitary currents evoked by 30 μM of glycine applied on outside-out patches excised from DA neurones of neonatal (*A*, postnatal day (P)7–P10), intermediate (*B*, P13–P16) and juvenile rats (*C*, P19–P22). The amplitude histograms shown in *A*, *B* and *C* were obtained by pooling recording epochs of 25–50 s from 13, 11 and 5 patches, respectively. Amplitude histograms were best fitted to the sum of three or four Gaussian functions, and mean amplitude and relative area (in parentheses) were indicated for each Gaussian function including the baseline (see Methods). Conductance levels were determined from the mean amplitude of each Gaussian function with E_{Cl} = −2 mV (V_H = −70 mV). Amplitude histograms were normalized using the current amplitude distribution corresponding to the baseline. Analysed recordings were sampled at 25 kHz and filtered at 2 kHz. The bin width is 0.1 pA.

Lack of strychnine-sensitive spontaneous IPSCs in DA neurones

The late switch from homomeric to heteromeric GlyRs observed in DA neurones could be correlated to the occurrence of a physiological activation process of GlyRs. We thus investigated whether any physiological release of agonists (glycine and/or taurine) could activate the GlyRs in DA neurones during postnatal development. Spontaneous IPSCs were studied in DA neurones in slices from neonatal and juvenile rats. In order to increase agonist release, most recordings (21/30) were performed with an extracellular solution containing 10 mM potassium. In the presence of the glutamatergic receptor antagonists DL-APV (50 μM) and CNQX (10 μM), DA neurones exhibited spontaneous activity (Fig. 6, left traces) both in neonatal (*A*) and juvenile rats (*B*). This activity was fully blocked by application of gabazine (2 μM), a specific $GABA_A$ receptor antagonist (middle traces), with no effect on glycine-evoked responses when applied at concentrations below 10 μM (Hussy *et al.* 1997; Mori *et al.* 2002). Application of 1 μM strychnine (right traces) had no further effect on basal current or baseline noise ($n = 27$). At this concentration, strychnine had no significant effect on GABA-evoked responses (Hussy *et al.* 1997; Mori *et al.* 2002).

Lack of taurine-mediated GlyR activation in DA neurones

Several lines of evidence suggest that taurine could be the endogenous ligand of GlyRs in the SNc and could be co-released with GABA (Clarke *et al.* 1983; Allen *et al.* 1986; Bianchi *et al.* 1998). To test whether GlyRs could be co-activated with $GABA_A$ receptors in response to the activation of GABA afferents surrounding DA neurones, IPSCs

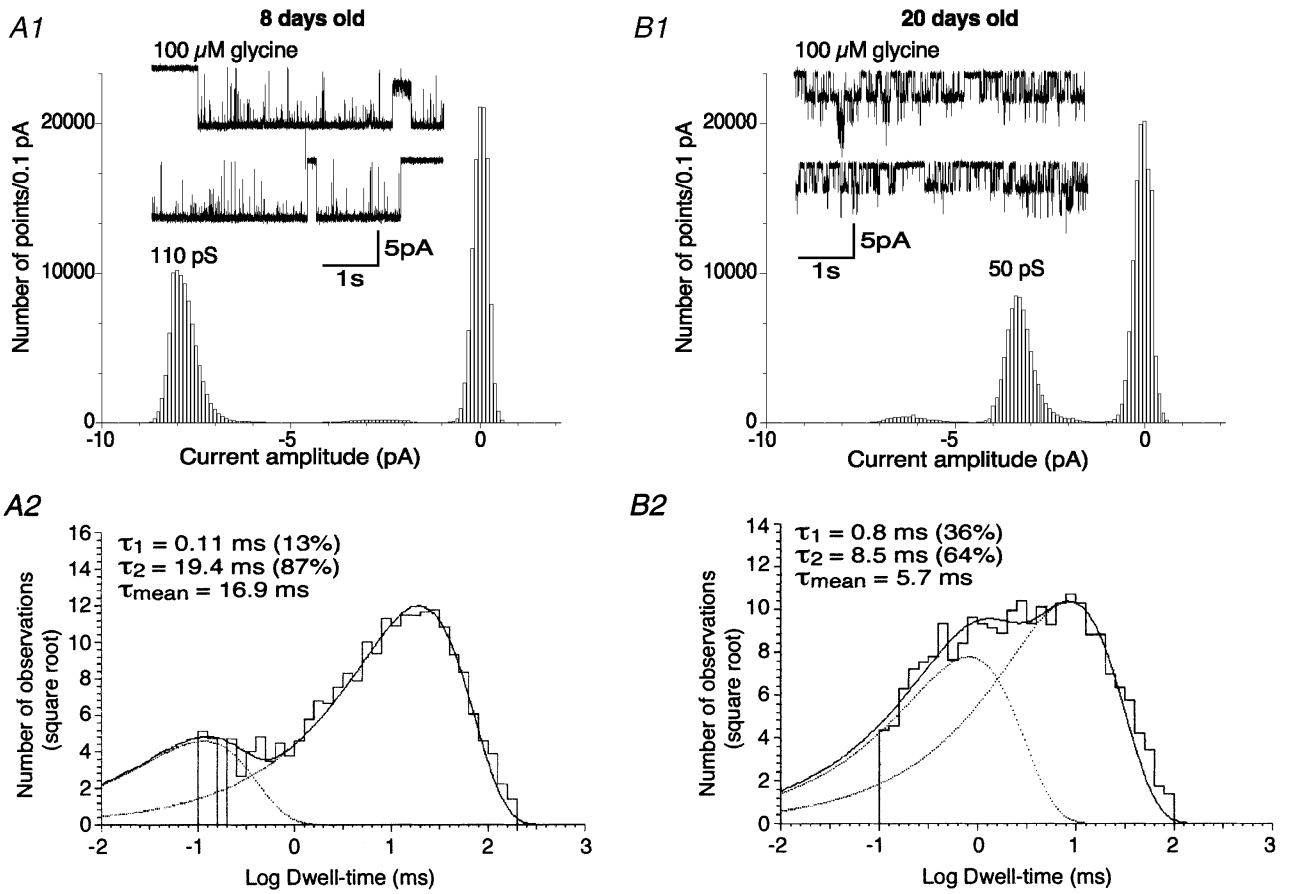

Figure 3. Gating properties of GlyRs expressed by SNc DA neurones in neonatal and juvenile rats

*A*1 and *B*1, examples of recordings obtained at P8 (*A*1) and P20 (*B*1) in response to 100 μM glycine ($V_H = -70$ mV). Corresponding point-per-point amplitude histograms were obtained from the epochs of 10 s displayed. Recordings were digitized at 25 kHz and filtered at 2 kHz. Currents larger than 5 pA in histogram *B*1 correspond to superimposed openings, as shown in the inset. *A*2 and *B*2, dwell-time histograms of the main open state observed in response to 100 μM glycine in neonatal (*A*2) and juvenile rats (*B*2). Histograms were obtained by analysing 50 s epochs obtained from the representative patches shown in *A*1 for neonatal rats and in *B*1 for juvenile rats. Histograms were best fitted with the sum of two exponential curves with time constants (τ) and proportions as indicated (see Methods). Outside-out recordings were digitized at 25 kHz and filtered at 3 kHz.

evoked by electrical stimulation of the GABAergic fibres were recorded in the presence of glutamatergic antagonists (DL-APV 50 μM, CNQX 10 μM). To optimize the taurine co-release with GABA from GABAergic terminals, we looked systematically for the best location around the recorded neurone to obtain the highest evoked synaptic current. Recordings were performed on both neonatal rats between P6 and P9 and on juvenile rats between P19 and P21. Evoked IPSC amplitudes (Fig. 7) were not significantly different between neonates and juveniles (respectively 509 ± 308 pA, $n = 30$ and 708 ± 547 pA, $n = 14$; unpaired t test, $P > 0.05$). By contrast, the half-width duration of GABAergic IPSCs was significantly shorter in juveniles (11 ± 2 ms, $n = 14$) compared to neonates (31 ± 7 ms, $n = 30$; unpaired t test, $P < 0.01$), due to a decrease in the deactivation time constants. At both ages, deactivation phases could be fitted by a double exponential function (see Methods). In neonatal rats, the deactivation time constants τ_{slow} and τ_{fast} were 117 ± 79 ms (weight of 35 ± 11 %) and 23 ± 8 ms ($n = 30$), respectively. In juveniles compared to neonates, the two deactivation time constants were significantly shorter (unpaired t test, $P < 0.01$): τ_{slow} was 46 ± 19 ms and τ_{fast} was 11 ± 3 ms ($n = 14$). However, the relative weights of these two deactivation components were not significantly different between neonates (τ_{slow}: 35 ± 11 %) and juveniles (τ_{slow}: 23 ± 7 %; unpaired t test, $P > 0.05$). These observations suggest that a maturation process also occurred at GABAergic synapses during this

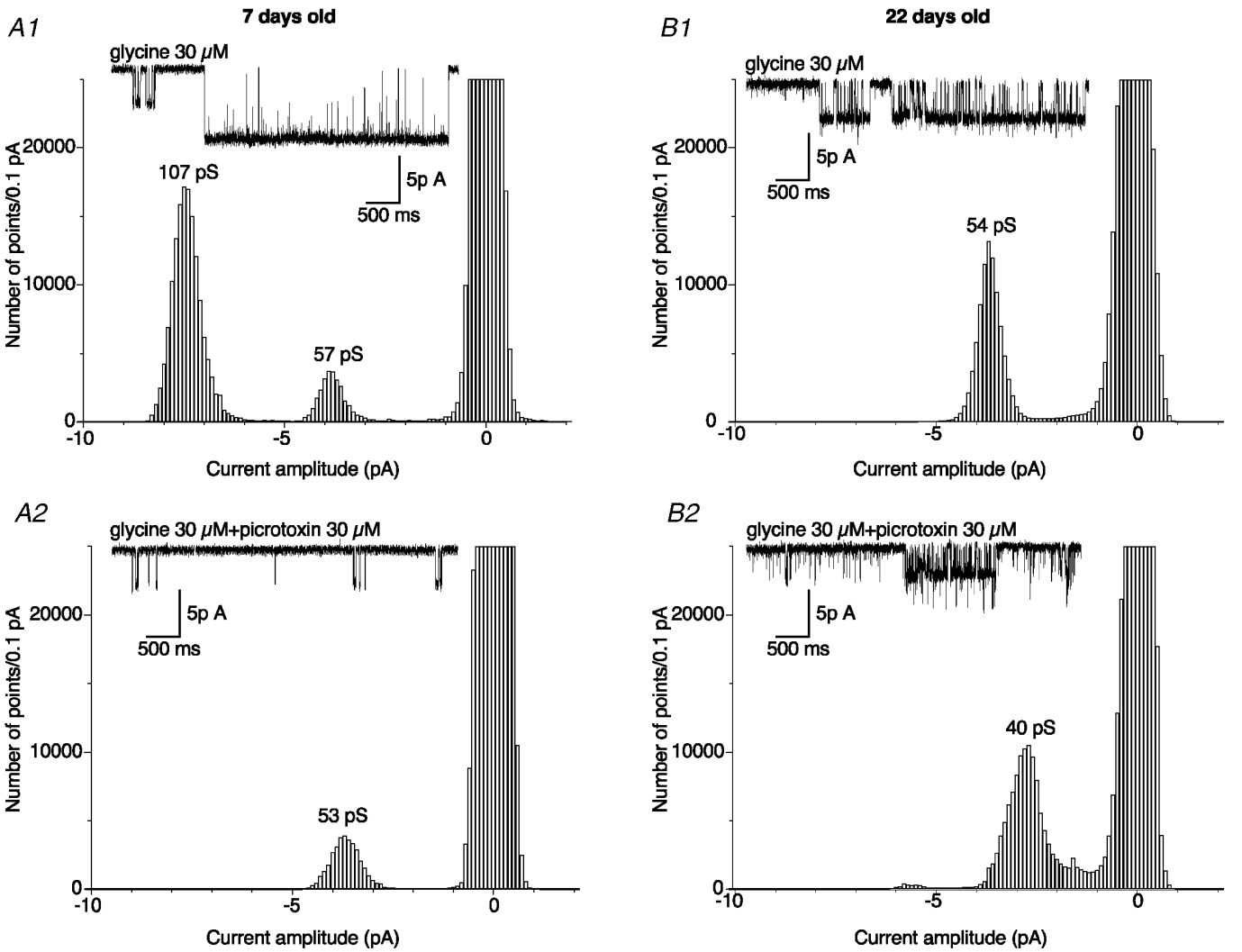

Figure 4. Differential effects of 30 μM picrotoxin on unitary currents evoked by glycine in neonatal and juvenile rats

Point-per-point amplitude histograms of single-channel currents evoked by 30 μM glycine alone (*A*1 and *B*1) and in the presence of 30 μM picrotoxin (*A*2 and *B*2) in neonatal (*A*1 and *A*2) and juvenile rats (*B*1 and *B*2). Amplitude histograms were obtained from 50 s recordings in each condition (bin width = 0.1 pA). Example traces of each recording are illustrated in the insets (2 kHz cut-off frequency; $V_H = -70$ mV). Note that in the presence of 30 μM picrotoxin, the unitary conductance of the GlyR was decreased from 54 to 40 pS in the patch excised from a P22 rat (*B*1 and *B*2). Currents larger than 5 pA in histogram *B*2 correspond to superimposed openings as shown in the inset.

period. Application of gabazine (1 μM; Fig. 7) almost completely suppressed the evoked IPSCs (97 ± 2 %; $n = 28$). Even train stimuli (see Methods) failed to reveal any putative GlyR activation in neonates ($n = 7$) and in juveniles ($n = 5$). The remaining current was not significantly modified by the subsequent application of strychnine (1 and 2 μM) either in neonates ($n = 20$) or in juveniles ($n = 8$).

To avoid possible taurine depletion, slices were pre-incubated in the presence of 1 μM taurine ($n = 7$; Hussy *et al.* 2001). We also used thicker slices (350 μM) in the horizontal plane ($n = 5$) with the aim of best preserving striatonigral afferents, which have been reported to release taurine in the substantia nigra (Clarke *et al.* 1983; Bianchi *et al.* 1998). Finally, some of the thick slices were pre-incubated in a medium containing 1 μM taurine ($n = 4$). However, both taurine pre-incubation and/or thick horizontal slices failed to reveal a strychnine-sensitive component in response to the electrical stimulation of the GABA afferents surrounding DA neurones.

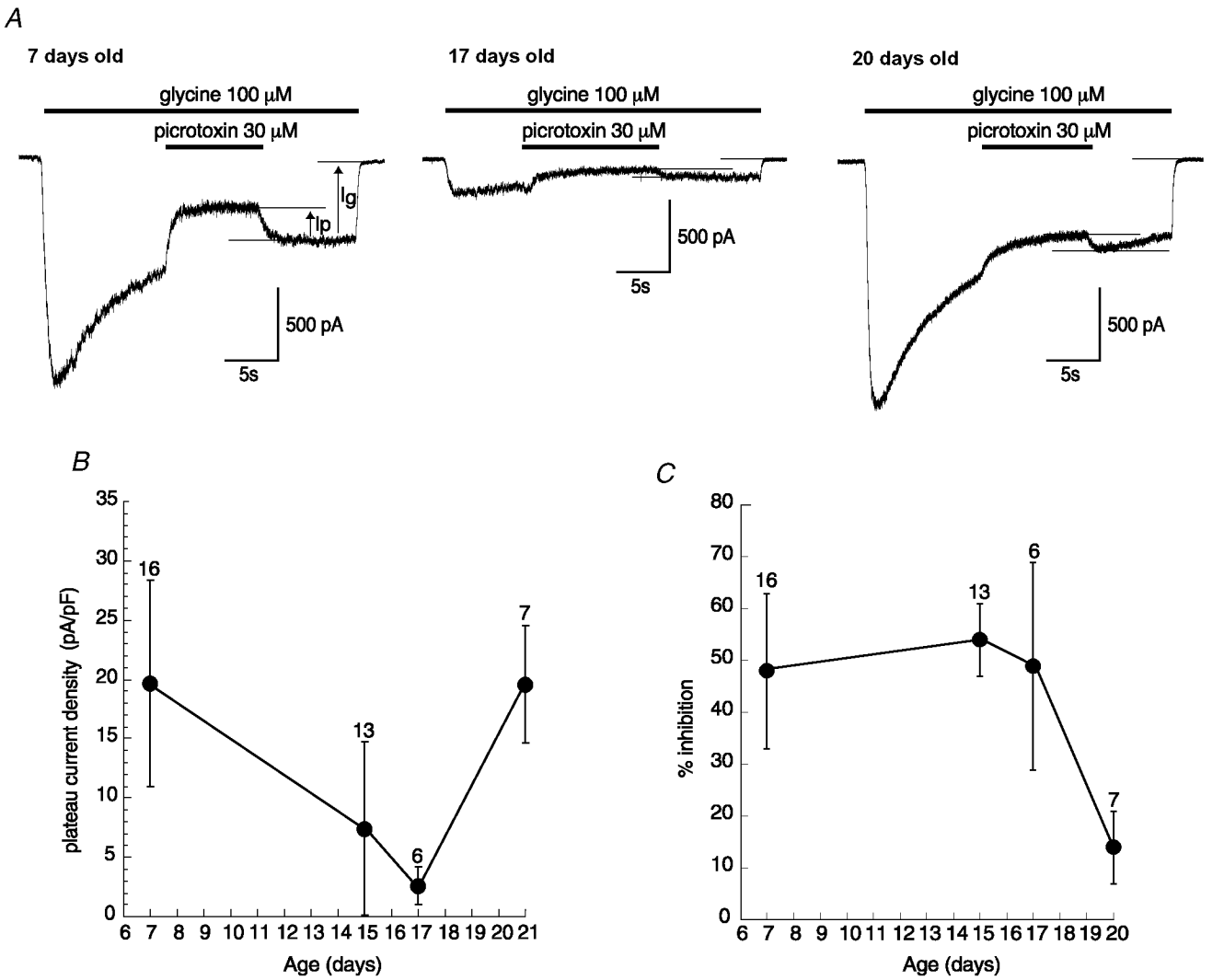

Figure 5. Developmental changes in the amplitude of glycine-evoked whole-cell currents and in their sensitivity to picrotoxin

A, examples of whole-cell currents evoked by 100 μM glycine and their inhibition by the transient application of 30 μM picrotoxin at three developmental stages ($V_H = -70$ mV). Traces were digitized at 10 kHz and filtered at 1 kHz. *B*, changes in the current density amplitude measured at the plateau current evoked by 100 μM glycine (Ig) at different developmental stages (mean amplitudes ± S.D., number of neurones tested given above). The current density amplitudes measured at P15 and P17 were significantly lower than those measured at P7 and P20 (ANOVA-DMCT, $P < 0.001$). *C*, changes in the percentage inhibition of the current evoked by 100 μM glycine in response to 30 μM picrotoxin applications at different ages. The percentage inhibition is calculated as the ratio of the current decrease in the presence of picrotoxin (Ip) to Ig. Mean ± S.D. The percentage inhibition at P20 was significantly lower than at P7, P15 and P17 (ANOVA-DMCT, $P < 0.001$).

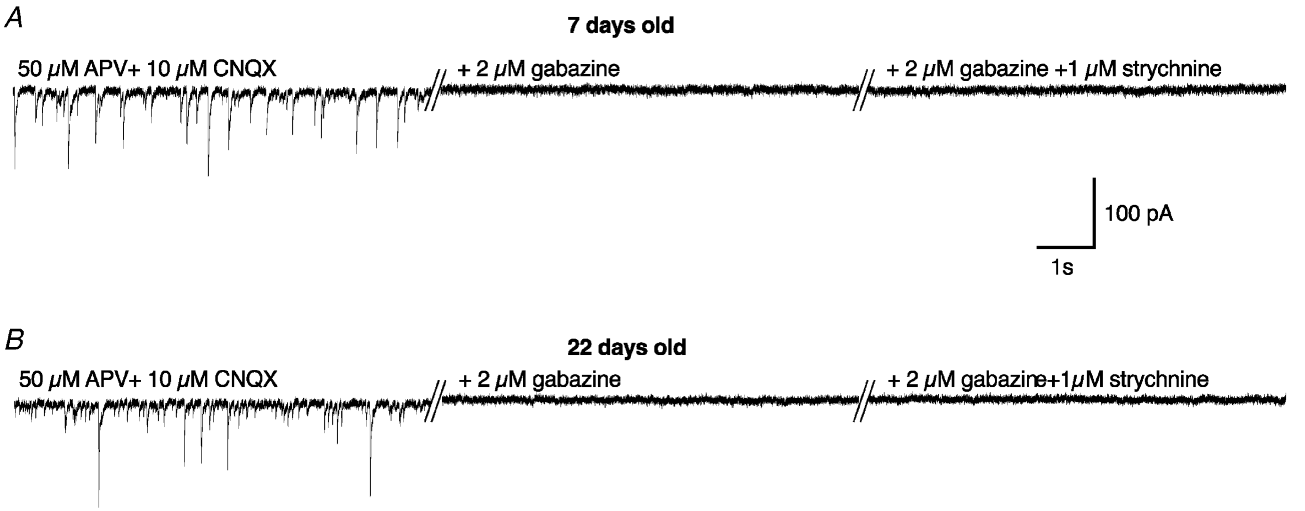

Figure 6. Absence of glycinergic spontaneous IPSCs or tonic glycinergic currents in neonatal and juvenile rats

Examples of spontaneous IPSCs recorded in DA neurones of the SNc at P7 (*A*) and P22 (*B*) in the presence of glutamatergic antagonists alone (50 μM DL-APV + 10 μM CNQX, left traces), added with a $GABA_A$ antagonist (middle traces) and after subsequent addition of a glycinergic antagonist (+ 1 μM strychnine, right traces). Traces were digitized at 10 kHz and filtered at 1 kHz (V_H = −70 mV).

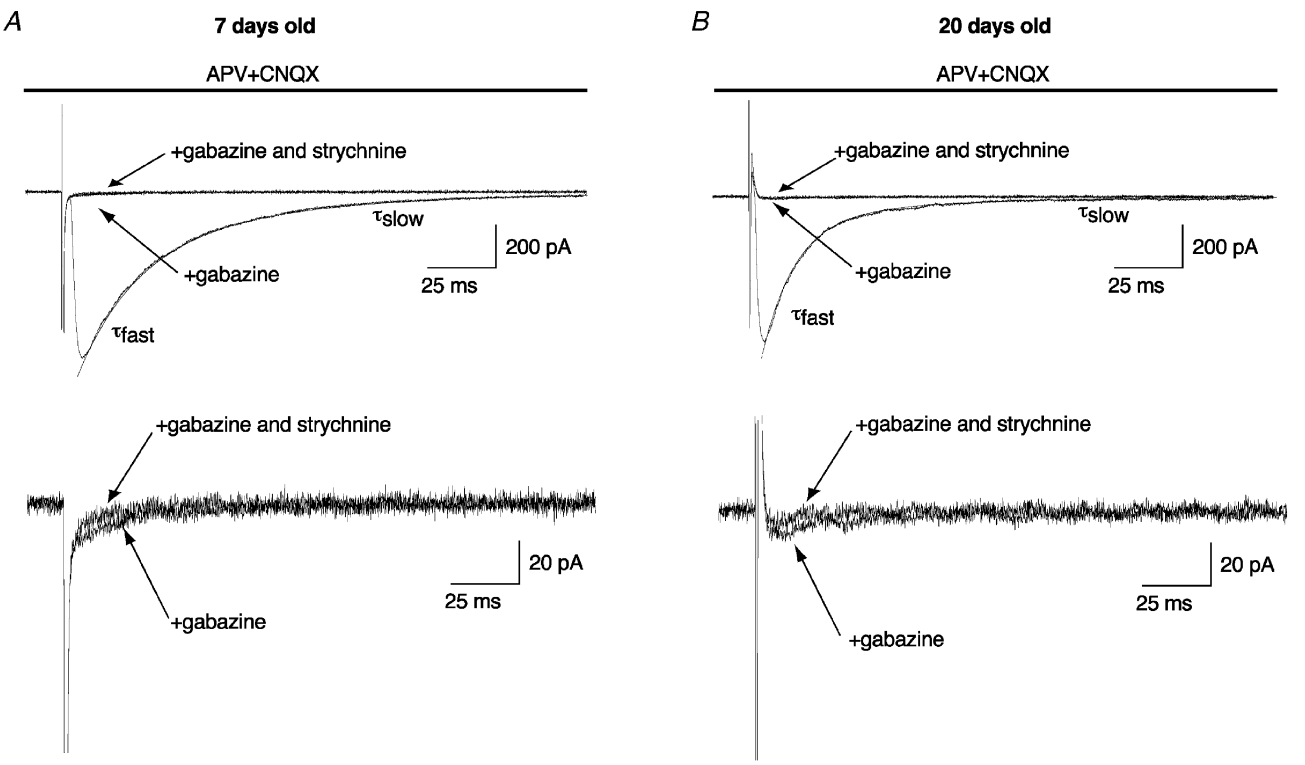

Figure 7. Electrical stimulation of DA neurone afferents fails to evoke any glycinergic IPSCs

Evoked IPSCs obtained in DA neurones recorded in neonatal (*A*) and juvenile rats (*B*). In the presence of glutamatergic antagonists (50 μM DL-APV + 10 μM CNQX), note that the addition of a $GABA_A$ antagonist (1 μM gabazine) inhibited the evoked IPSCs. Subsequent addition of strychnine (1 μM) had little effect on the remaining current (approximately 5 pA, lower traces). Traces were digitized at 10 kHz and filtered at 1 kHz. Lower traces are a magnification of upper traces (V_H = −70 mV).

In addition, we tried to reveal an endogenous but subthreshold taurine release by blocking taurine uptake. Focal application of the taurine uptake blocker GES (300 μM) on DA neurones induced an inward current of 140 ± 64 pA, which was reduced to 18 ± 6 pA in the presence of 1 μM gabazine and was almost fully blocked by 10 μM gabazine (n = 5, Fig. 8*A*). Application of 100 μM GES on patches excised from DA neurones induced single-channel openings exhibiting a main conductance of 24 pS that were almost fully blocked by 1 μM gabazine (n = 4, Fig. 8*B*1 and *B*2). Our results confirm that GES, in addition to the blockade of taurine uptake, exerts an agonist action on $GABA_A$ receptors, as shown previously (Mellor *et al.* 2000). Furthermore, the current induced by 300 μM GES in the presence of 1 μM gabazine was strychnine-insensitive (1 μM strychnine, n = 8, Fig. 8*C*). Thus, no GlyR activation can be induced by the blockade of taurine uptake.

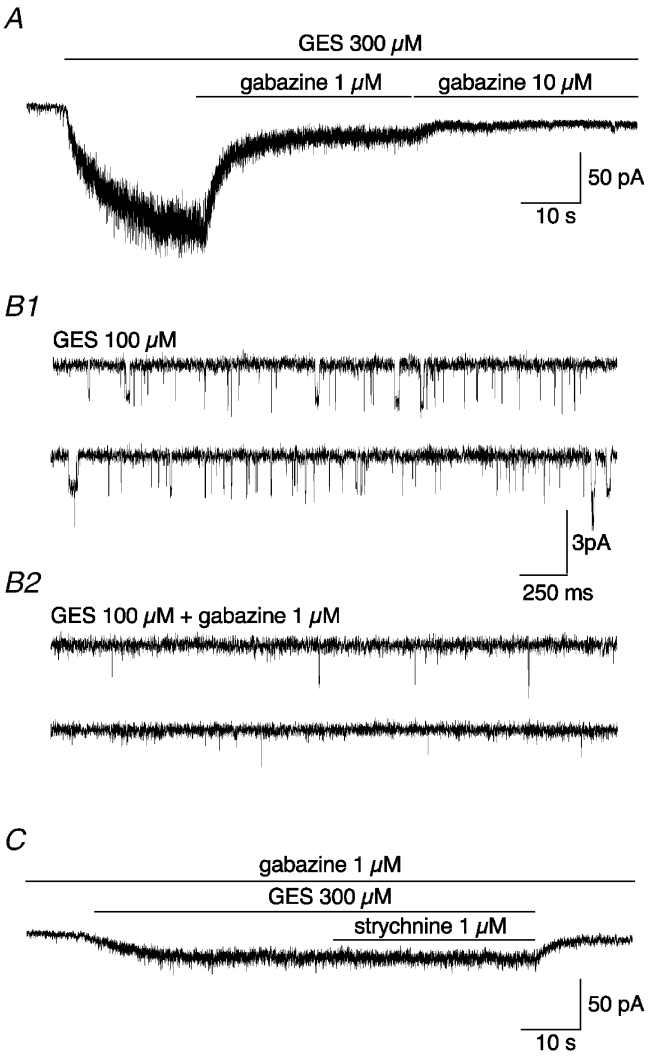

Figure 8. The inward current induced by guanidinoethyl sulfonate (GES) in DA neurones is mediated by $GABA_A$ receptors

A, example of inward currents evoked by the focal application of 300 μM GES on a DA neurone. Note that this current can be completely inhibited by the application of 10 μM gabazine, a specific $GABA_A$ receptor antagonist (see Results). The trace was digitized at 10 kHz and filtered at 500 Hz. *B*1 and *B*2, example of single-channel currents evoked by 100 μM GES in a patch excised from a DA neurone (*B*1). The main conductance level of the single channels was 24 pS. Note that single-channel activity was dramatically reduced by 1 μM gabazine application (*B*2). Traces were digitized at 25 kHz and filtered at 1 kHz. *C*, the residual whole-cell current observed in the presence of 300 μM GES + 1 μM gabazine was insensitive to 1 μM strychnine application. The trace was digitized at 10 kHz and filtered at 500 Hz.

Finally, as it has been shown that during fetal and early postnatal development, GlyRs expressed by immature neocortical neurones can be activated via a non-synaptic pathway by taurine release in response to hyposmotic shock (Flint *et al.* 1998), this possibility was also tested. Hyposmotic stimulation using low-osmolarity PBBS was performed on DA neurones from neonatal rats (P6–P10). In the presence of DL-APV (50 μM), CNQX (10 μM) and gabazine (1 μM), local application of 270 mosmol l^{-1} PBBS or 200 mosmol l^{-1} PBBS had no effect on whole-cell current baseline (n = 5, data not shown).

DISCUSSION

We have characterized the electrophysiological properties of GlyRs in DA neurones of the SNc during postnatal development in rats. Our results show that the glycine responses in DA neurones of neonatal rats (P6–P10) are characteristic of α_2 homomeric GlyRs, whereas those of DA neurones of juvenile rats (P19–P22) most resemble α_1/β heteromeric GlyRs. The switch between these two functional phenotypes occurs during a transient period of insensitivity of DA neurones to glycine, which probably corresponds to a gap in GlyR expression. Because the physiological significance of the presence of GlyR in DA neurones remains unknown, several experiments were performed to explore it. However, spontaneous or stimulation-evoked glycinergic or taurinergic synaptic transmission was never observed, suggesting that GlyR maturation in DA neurones of the SNc occurs independently of any obvious physiological activation and would instead be correlated to the general maturation of DA neurones at this time.

GlyR subtype expression during postnatal development in DA neurones

A switch from the neonatal α_2 to the adult α_1 subunit has been described in many brain structures during the first two postnatal weeks in the rat (Akagi & Miledi, 1988; Malosio *et al.* 1991). This switch is correlated with a decrease in the GlyR mean open time and in the glycinergic IPSC decay time in spinal cord (Takahashi *et al.* 1992) and brainstem neurones (Singer *et al.* 1998). Our results suggest that the same switch in subunit type from α_2 to α_1 occurs in DA neurones of the SNc. Between P7 and P16, the maximal conductance level observed shifts from level I

(100–110 pS) to level II (80–90 pS), which corresponds to the main conductance states measured when HEK-393 cells are transfected with the α_2 and α_1 homomeric GlyR, respectively (Bormann *et al.* 1993). In addition, we observed a decrease in the GlyR mean open time between P6 and P20 in DA neurones. This decrease suggests further the functional replacement of α_2- by α_1-containing GlyRs in DA neurones during this period, considering the longer mean open time of α_2-containing GlyRs compared to α_1-containing GlyRs (Takahashi *et al.* 1992).

In spinal and brainstem neurones, GlyR maturation also involves a switch from α homomeric to α/β heteromeric GlyR expression. This phenomenon is considered to be critical for GlyR location at synapses, since only GlyR β subunits can bind to the gephyrin postsynaptic submembrane protein (Kirsch *et al.* 1995; Meyer *et al.* 1995). Our study supports in several ways the existence of a similar switch in DA neurones of the SNc. First, the relative occurrence of high-conductance levels (> 55 pS), frequently observed between P6 and P16, is greatly reduced in patches excised from P19–P22 rats. Simultaneously, the picrotoxin sensitivity of glycine-evoked currents falls after P17, both in outside-out and whole-cell recordings. Taken together, these results support the hypothesis that a functional switch from homomeric to heteromeric GlyRs also takes place in SNc DA neurones. Thus, this developmental regulation of GlyRs in SNc DA neurones is in accordance with the expression pattern observed in other CNS areas and/or cell types: rat spinal cord neurones in slices (Takahashi *et al.* 1992) and in cultures (Tapia & Aguayo, 1998), ventral tegmental area neurones (Ye, 2000), auditory brainstem neurones (Kungel & Friauf, 1997) and oligodendrocytes (Pastor *et al.* 1995; Belachew *et al.* 1998).

GlyR maturation in DA neurones of the SNc does not require the presence of glycinergic terminals or GlyR activation

It has been hypothesized that in spinal cord and brainstem, the origin of the switch from α_2 homomeric to α_1/β heteromeric GlyRs is correlated with the maturation of glycinergic synapses (Takahashi *et al.* 1992; Singer *et al.* 1998). However, our results suggest that such glycinergic inputs are absent in the DA neurones of the SNc. Despite strong GABAergic activity, indicating a healthy afferent system, we did not record any spontaneous or evoked glycinergic or taurinergic IPSCs, even when using protocols known to facilitate neurotransmitter release. This is consistent with the reported absence of the synaptic glycine transporter GLYT2 (Zafra *et al.* 1995) and the very poor glycine immunoreactivity of fibres observed in the substantia nigra (Rampon *et al.* 1996). Other studies have suggested a possible taurinergic neurotransmission in the SNc (Clarke *et al.* 1983; Allen *et al.* 1986) via the co-release of taurine with GABA from striatonigral afferents (Bianchi *et al.* 1996, 1998). Therefore, our inability to detect any GlyR activation by taurine was surprising. To be activated by this GABA/taurine co-release, GlyRs must aggregate at postsynaptic sites apposed to GABAergic inputs. The submembrane anchoring protein gephyrin is also known to interact with $GABA_A$ receptors (Kneussel & Betz, 2000) and it was proposed to account for the co-aggregation of $GABA_A$ receptors and GlyRs at synapses co-releasing GABA and glycine (Todd *et al.* 1996; O'Brien & Berger, 1999; Dumoulin *et al.* 2001). However, GlyRs must contain a β subunit to interact with gephyrin (Kirsch *et al.* 1995; Meyer *et al.* 1995). Therefore, it seems unlikely that the α homomeric GlyRs detected before P17 can accumulate at GABAergic synapses. However, we cannot exclude that α/β heteromeric GlyRs present in the most mature DA neurones could be aggregated at GABAergic synapses. In this case, the lack of GlyR activation by GABAergic fibre stimulation suggests that the amount of taurine released is insufficient, especially in a mature brain where taurine concentration levels are much lower than in the fetal brain (Sturman, 1988; Flint *et al.* 1998), and/or that GlyRs aggregate at the periphery of GABAergic synapses, far from the vesicular release sites.

GlyR maturation seems to follow the general maturation scheme of SNc DA neurones

Despite the good accordance observed between the functional expression pattern of GlyRs in the SNc and in lower brain structures, the functional switch from homomeric to heteromeric GlyRs occurs in the SNc at around P17, 2 weeks later than in the spinal cord. In the spinal cord, this developmental period is correlated with the maturation of motoneurones: around birth, there is a peak of multi-innervation of muscles by motoneurones, which precedes the synapse elimination and maturation of motor network that occurs during postnatal development (Brown *et al.* 1976; Rosenthal & Taraskevich, 1977). In DA neurones of the rat SNc, there are converging arguments suggesting that the switch from homomeric to heteromeric GlyRs also occurs during a period of neuronal differentiation (Voorn *et al.* 1988; Tepper *et al.* 1994) and apoptosis (Janec & Burke, 1993; Oo & Burke, 1997). After a transient phase of pacemaker-like activity around P15 (Tepper *et al.* 1990), DA neurones acquire a firing pattern and a morphology close to their adult profile during the 3rd postnatal week (Tepper *et al.* 1990, 1994; Washio *et al.* 1999). At the same time, a peak in neuronal apoptosis is also observed within the SNc (Oo & Burke, 1997), while the number of synapses greatly increases in the developing striatum (Hamill *et al.* 1983), suggesting a transient dependence of DA neurones on their striatal target at this developmental stage (Marti *et al.* 1997). At this time we observed a decrease in the decay time of GABA IPSCs evoked by electrical stimulation, a phenomenon that has been shown in many brain structures to reflect a switch from the α_2 to α_1 subunit of the $GABA_A$ receptor (Brussaard *et al.* 1997; Okada *et al.* 2000; Vicini *et al.* 2001). Therefore, the switch from

homomeric to heteromeric GlyRs occurs simultaneously with an important phase of maturation in SNc DA neurones. This observation could be generalized to other neuronal populations such as spinal and brainstem motoneurones, where the switch from homomeric to heteromeric GlyRs occurs around birth during an important phase in motor network maturation (Becker *et al.* 1988; Malosio *et al.* 1991; Takahashi *et al.* 1992). Therefore, rather than being associated directly with the establishment of the glycinergic synapse, the switch from homomeric to heteromeric GlyRs could be linked to the general maturation processes occurring within the same period.

In conclusion, our results demonstrate that the functional switch from homomeric α_2 to heteromeric α_1/β GlyRs occurs independently of any synaptic GlyR stimulation in the SNc. This could also be the case in other brain areas where glycinergic synapses are present. Thus, the switch in GlyR expression may be distinguished from the maturation of the glycinergic postsynaptic specialization, which requires the presence of functional presynaptic glycine fibres (Kneussel & Betz, 2000).

REFERENCES

Akagi, H. & Miledi, R. (1988). Heterogeneity of glycine receptors and their messenger RNAs in rat brain and spinal cord. *Science* **242**, 270–273.

Ali, D. W., Drapeau, P. & Legendre, P. (2000). Development of spontaneous glycinergic currents in the Mauthner neuron of the zebrafish embryo. *Journal of Neurophysiology* **84**, 1726–1736.

Allen, I. C., Grieve, A. & Griffiths, R. (1986). Differential changes in the content of amino acid neurotransmitters in discrete regions of the rat brain prior to the onset and during the course of homocysteine-induced seizures. *Journal of Neurochemistry* **46**, 1582–1592.

Becker, C. M., Hoch, W. & Betz, H. (1988). Glycine receptor heterogeneity in rat spinal cord during postnatal development. *EMBO Journal* **7**, 3717–3726.

Belachew, S., Rogister, B., Rigo, J. M., Malgrange, B., Mazy-servais, C., Xhauflaire, G., Coucke, P. & Moonen, G. (1998). Cultured oligodendrocyte progenitors derived from cerebral cortex express a glycine receptor which is pharmacologically distinct from the neuronal isoform. *European Journal of Neuroscience* **10**, 3556–3564.

Bianchi, L., Bolam, J. P., Galeffi, F., Frosini, M., Palmi, M., Sgaragli, G. & Della Corte, L. (1996). *In vivo* release of taurine from rat neostriatum and substantia nigra. *Advances in Experimental Medicine and Biology* **403**, 427–433.

Bianchi, L., Colivicchi, M. A., Bolam, J. P. & Della Corte, L. (1998). The release of amino acids from rat neostriatum and substantia nigra *in vivo*: a dual microdialysis probe analysis. *Neuroscience* **87**, 171–180.

Bormann, J., Rundstrom, N., Betz, H. & Langosch, D. (1993). Residues within transmembrane segment M2 determine chloride conductance of glycine receptor homo- and hetero-oligomers (erratum appears in *EMBO Journal* **13**, 1493 (1994)). *EMBO Journal* **12**, 3729–3737.

Brown, M. C., Jansen, J. K. & Van Essen, D. (1976). Polyneuronal innervation of skeletal muscle in new-born rats and its elimination during maturation. *Journal of Physiology* **261**, 387–422.

Brussaard, A. B., Kits, K. S., Baker, R. E., Willems, W. P., Leyting-Vermeulen, J. W., Voorn, P., Smit, A. B., Bicknell, R. J. & Herbison, A. E. (1997). Plasticity in fast synaptic inhibition of adult oxytocin neurons caused by switch in GABA(A) receptor subunit expression. *Neuron* **19**, 1103–1114.

Clarke, D. J., Smith, A. D. & Bolam, J. P. (1983). Uptake of [^{3}H]taurine into medium-size neurons and into identified striatonigral neurons in the rat neostriatum. *Brain Research* **289**, 342–348.

Dumoulin, A., Triller, A. & Dieudonne, S. (2001). IPSC kinetics at identified GABAergic and mixed GABAergic and glycinergic synapses onto cerebellar Golgi cells. *Journal of Neuroscience* **21**, 6045–6057.

Flint, A. C., Liu, X. & Kriegstein, A. R. (1998). Nonsynaptic glycine receptor activation during early neocortical development. *Neuron* **20**, 43–53.

Hamill, O. P., Bormann, J. & Sakmann, B. (1983). Activation of multiple-conductance state chloride channels in spinal neurones by glycine and GABA. *Nature* **305**, 805–808.

Hausser, M. A., Yung, W. H. & Lacey, M. G. (1992). Taurine and glycine activate the same Cl^- conductance in substantia nigra dopamine neurones. *Brain Research* **571**, 103–108.

Hussy, N., Bres, V., Rochette, M., Duvoid, A., Alonso, G., Dayanithi, G. & Moos, F. C. (2001). Osmoregulation of vasopressin secretion via activation of neurohypophysial nerve terminals glycine receptors by glial taurine. *Journal of Neuroscience* **21**, 7110–7116.

Hussy, N., Deleuze, C., Pantaloni, A., Desarmenien, M. G. & Moss, F. (1997). Agonist action of taurine on glycine receptors in rat supraoptic magnocellular nucleus: possible role in osmoregulation. *Journal of Physiology* **502**, 609–621.

Janec, E. & Burke, R. E. (1993). Naturally occurring cell death during postnatal development of the substantia nigra pars compacta of rat. *Molecular and Cellular Neurosciences* **4**, 30–35.

Kaneda, M., Farrant, M. & Cull-Candy, S. G. (1995) Whole-cell and single-channel currents activated by GABA and glycine in granule cells of the rat cerebellum. *Journal of Physiology* **485**, 419–435.

Kirsch, J., Kuhse, J. & Betz, H. (1995). Targeting of glycine receptor subunits to gephyrin-rich domains in transfected human embryonic kidney cells. *Molecular and Cellular Neurosciences* **6**, 450–461.

Kneussel, M. & Betz, H. (2000). Clustering of inhibitory neurotransmitter receptors at developing postsynaptic sites: the membrane activation model. *Trends in Neurosciences* **23**, 429–435.

Kungel, M. & Friauf, E. (1997). Physiology and pharmacology of native glycine receptors in developing rat auditory brainstem neurons. *Brain Research Developmental Brain Research* **102**, 157–165.

Langosch, D., Thomas, L. & Betz, H. (1988). Conserved quaternary structure of ligand-gated ion channels: the postsynaptic glycine receptor is a pentamer. *Proceedings of the National Academy of Sciences of the USA* **85**, 7394–7398.

Legendre, P. (1997). Pharmacological evidence for two types of postsynaptic glycinergic receptors on the Mauthner cell of 52-h-old zebrafish larvae. *Journal of Neurophysiology* **77**, 2400–2415.

Legendre, P. (2001). The glycinergic inhibitory synapse. *Cellular and Molecular Life Sciences* **58**, 760–793.

Legendre, P. & Korn, H. (1994). Glycinergic inhibitory synaptic currents and related receptor channels in the zebrafish brain. *European Journal of Neuroscience* **6**, 1544–1557.

Lynch, J. W., Rajendra, S., Barry, P. H. & Schofield, P. R. (1995). Mutations affecting the glycine receptor agonist transduction mechanism convert the competitive antagonist, picrotoxin, into an allosteric potentiator. *Journal of Biological Chemistry* **270**, 13799–13806.

Malosio, M. L., Marqueze-Pouey, B., Kuhse, J. & Betz, H. (1991). Widespread expression of glycine receptor subunit mRNAs in the adult and developing rat brain. *EMBO Journal* **10**, 2401–2409.

Marti, M. J., James, C. J., Oo, T. F., Kelly, W. J. & Burke, R. E. (1997). Early developmental destruction of terminals in the striatal target induces apoptosis in dopamine neurons of the substantia nigra. *Journal of Neuroscience* **17**, 2030–2039.

Mellor, J. R., Gunthorpe, M. J. & Randall, A. D. (2000). The taurine uptake inhibitor guanidinoethyl sulphonate is an agonist at γ-aminobutyric acid$_A$ receptors in cultured murine cerebellar granule cells. *Neuroscience Letters* **286**, 25–28.

Mercuri, N. B., Calabresi, P. & Bernardi, G. (1988). Potassium ions play a role in the glycine-induced inhibition of rat substantia nigra zona compacta neurones. *Brain Research* **462**, 199–203.

Meyer, G., Kirsch, J., Betz, H. & Langosch, D. (1995). Identification of a gephyrin binding motif on the glycine receptor beta subunit. *Neuron* **15**, 563–572.

Mori, M., Gahwiler, B. H. & Gerber, U. (2002). β-Alanine and taurine as endogenous agonists at glycine receptors in rat hippocampus *in vitro*. *Journal of Physiology* **539**, 191–200.

O'brien, J. A. & Berger, A. J. (1999). Cotransmission of GABA and glycine to brain stem motoneurons. *Journal of Neurophysiology* **82**, 1638–1641.

Okada, M., Onodera, K., Van Renterghem, C., Sieghart, W. & Takahashi, T. (2000). Functional correlation of GABA(A) receptor alpha subunits expression with the properties of IPSCs in the developing thalamus. *Journal of Neuroscience* **20**, 2202–2208.

Oo, T. F. & Burke, R. E. (1997). The time course of developmental cell death in phenotypically defined dopaminergic neurons of the substantia nigra. *Brain Research Developmental Brain Research* **98**, 191–196.

Pastor, A., Chvatal, A., Sykova, E. & Kettenmann, H. (1995). Glycine- and GABA-activated currents in identified glial cells of the developing rat spinal cord slice. *European Journal of Neuroscience* **7**, 1188–1198.

Pitha, J. (1985). Amorphous water-soluble derivatives of cyclodextrins: nontoxic dissolution enhancing excipients. *Journal of Pharmaceutical Sciences* **74**, 987–990.

Pribilla, I., Takagi, T., Langosch, D., Bormann, J. & Betz, H. (1994). The atypical M2 segment of the beta subunit confers picrotoxinin resistance to inhibitory glycine receptor channels. *EMBO Journal* **13**, 1493.

Rampon, C., Luppi, P. H., Fort, P., Peyron, C. & Jouvet, M. (1996). Distribution of glycine-immunoreactive cell bodies and fibers in the rat brain. *Neuroscience* **75**, 737–755.

Rosenthal, J. L. & Taraskevich, P. S. (1977). Reduction of multiaxonal innervation at the neuromuscular junction of the rat during development. *Journal of Physiology* **270**, 299–310.

Sigworth, F. J. & Sine, S. M. (1987). Data transformations for improved display and fitting of single-channel dwell time histograms. *Biophysical Journal* **52**, 1047–1054.

Singer, J. H., Talley, E. M., Bayliss, D. A. & Berger, A. J. (1998). Development of glycinergic synaptic transmission to rat brain stem motoneurons. *Journal of Neurophysiology* **80**, 2608–2620.

Sturman, J. A. (1988). Taurine in development. *The Journal of Nutrition* **118**, 1169–1176.

Takahashi, T., Momiyama, A., Hirai, K., Hishinuma, F. & Akagi, H. (1992). Functional correlation of fetal and adult forms of glycine receptors with developmental changes in inhibitory synaptic receptor channels. *Neuron* **9**, 1155–1161.

Tapia, J. C. & Aguayo, L. G. (1998). Changes in the properties of developing glycine receptors in cultured mouse spinal neurons. *Synapse* **28**, 185–194.

Tepper, J. M., Damlama, M. & Trent, F. (1994). Postnatal changes in the distribution and morphology of rat substantia nigra dopaminergic neurons. *Neuroscience* **60**, 469–477.

Tepper, J. M., Trent, F. & Nakamura, S. (1990). Postnatal development of the electrical activity of rat nigrostriatal dopaminergic neurons. *Brain Research Developmental Brain Research* **54**, 21–33.

Todd, A. J., Watt, C., Spike, R. C. & Sieghart, W. (1996). Colocalization of GABA, glycine, and their receptors at synapses in the rat spinal cord. *Journal of Neuroscience* **16**, 974–982.

Vannier, C. & Triller, A. (1997). Biology of the postsynaptic glycine receptor. *International Review of Cytology* **176**, 201–244.

Vicini, S., Ferguson, C., Prybylowski, K., Kralic, J., Morrow, A. L. & Homanics, G. E. (2001). GABA(A) receptor alpha1 subunit deletion prevents developmental changes of inhibitory synaptic currents in cerebellar neurons. *Journal of Neuroscience* **21**, 3009–3016.

Voorn, P., Kalsbeek, A., Jorritsma-Byham, B. & Groenewegen, H. J. (1988). The pre- and postnatal development of the dopaminergic cell groups in the ventral mesencephalon and the dopaminergic innervation of the striatum of the rat. *Neuroscience* **25**, 857–887.

Washio, H., Takigachi-Hayashi, K. & Konishi, S. (1999). Early postnatal development of substantia nigra neurons in rat midbrain slices: hyperpolarization-activated inward current and dopamine-activated current. *Neuroscience Research* **34**, 91–101.

Ye, J. (2000). Physiology and pharmacology of native glycine receptors in developing rat ventral tegmental area neurons. *Brain Research* **862**, 74–82.

Yoon, K. W., Wotring, V. E. & Fuse, T. (1998). Multiple picrotoxinin effect on glycine channels in rat hippocampal neurons. *Neuroscience* **87**, 807–815.

Zafra, F., Aragon, C., Olivares, L., Danbolt, N. C., Gimenez, C. & Storm-Mathisen, J. (1995). Glycine transporters are differentially expressed among CNS cells. *Journal of Neuroscience* **15**, 3952–3969.

Acknowledgements

This work was supported by the Centre National de la Recherche Scientifique, the Université Pierre et Marie Curie and the Ministère de la Recherche. We thank Jean-Michel Rigo and Anne Lohof for their helpful comments on this manuscript and Antoine Triller for valuable discussions on the experiments. We also wish to thank David Failli and Daniel Brusciano for their technical assistance and precious suggestions.